ChemComm

COMMUNICATION

View Article Online
View Journal | View Issue

Engineering the surface of perovskite $La_{0.5}Sr_{0.5}MnO_3$ for catalytic activity of CO oxidation†

Cite this: *Chem. Commun.*, 2014, 50, 9200

Received 2nd January 2014,
Accepted 25th June 2014

DOI: 10.1039/c4cc00023d

www.rsc.org/chemcomm

Keke Huang,[a] Xuefeng Chu,[b] Long Yuan,[a] Wenchun Feng,[c] Xiaofeng Wu,[a] Xiyang Wang[a] and Shouhua Feng*[a]

Published on 26 June 2014. Downloaded by Jilin University on 15/08/2017 03:09:29.

A simple treatment of $La_{0.5}Sr_{0.5}MnO_3$ with diluted HNO_3 creates more B-sites (rich) on the terminated perovskite surface and improves its catalytic activity toward CO oxidation, and the perovskite catalyst possesses a higher ratio of Mn^{4+}/Mn^{3+} and thus enhances the O_2 adsorption capability, favourable for CO oxidation and catalytic activity.

Design of efficient catalysts providing better-controlled active sites for fundamental studies of heterogenous catalysis and developing novel industrial catalysts is the ultimate goal of research on heterogeneous catalysis.[1] Generally, the size, shape, composition, and interface/surface engineering in catalytic materials are the key parameters that are usually considered in synthesis to exhibit the rule of catalyst dependence.[2,3] Since heterogeneous catalysis usually occurs on solid surfaces providing the approprite electronic and/or geometric environment, design of active sites on the surface requires precise control on the atomic scale.[1,4] As a promising candidate for the replacement of noble metals, which are commonly expensive and exhibit limited stability, perovskite oxides (especially La(Sr)MnO_3 and La(Sr)CoO_3) are emerging as automotive exhaust catalysts.[5,6] However, J. T. S. Irvine[7] reported that native perovskite surfaces are preferentially A-site (rich), not catalytically active sites,[8] terminated to the detriment of the B sites, which results in the true catalytic properties of many perovskites based on ideal bulk-like terminated surfaces which might have been underestimated due to their fundamental flaw. There is still a lack of fundamental understanding of the perovskite surface catalytic mechanism at the atomic/molecular level. To overcome these disadvantages, a clean procedure to create more B-site (rich) terminated perovskite surfaces and related catalytic property investigations are greatly in need.

Acid/base treatment of catalysts was regarded as one of the most widely accepted method to improve specific performance in porous TiO_2,[9] zeolites,[10] layered perovskites[11] and carbon materials.[12] Treatment with H_2O_2 and NH_4OH for modification of surface electronic and magnetic properies in perovskite films was also reported.[13] However, to date no work on the wet-etching treatment of perovskite catalysts has been reported for activating the perovskite.

Herein, we developed a method to modulate the perovskite surface of $La_{0.5}Sr_{0.5}MnO_3$ samples, *e.g.*, treatment of dilute HNO_3 solutions with controlled time followed by the evaluation of the corresponding catalytic activity for CO oxidation. Our finding demonstrates that the simple surface treatment shows the importance of B-site (rich) terminated perovskite surface control in harnessing the true catalytic potential of perovskite oxides and opens up strategies for the development of the activity for other perovskite transition-metal oxides.

The raw sample was synthesized *via* a hydrothermal route adapted from a previous report with minor modification.[14,15] The details of sample preparation and the acid activation process are given in the ESI.† Upon increasing treatment time, the crystal structure remains the same as the raw sample, which can be indexed to a primitive cubic unit cell (in Fig. 1 space group *Pm*3*m*, a = 3.841 Å). Inductively coupled plasma elemental analysis of the raw sample confirmed the energy dispersive spectrometry (EDS) result (inset of Fig. 3a) and indicated that its bulk composition is $La_{0.5}Sr_{0.5}MnO_3$. Usually, the yielded raw $La_{0.5}Sr_{0.5}MnO_3$ particles are La, Sr-enriched on the surface and this phenomenon of A-enriched in other perovskite systems often appears.[7,16–18] The surface composition changes from La, Sr-rich to Mn-rich by the modification of simple treatment by dilute HNO_3 solutions. Surface composition was evaluated by X-ray photoemission spectroscopy (XPS) which is a surface sensitive technique for probing the surface composition and the electronic structure.

[a] *State Key Laboratory of Inorganic Synthesis and Preparative Chemistry, College of Chemistry, Jilin University, Changchun 130012, P. R. China. E-mail: shfeng@mail.jlu.edu.cn; Fax: +86-431-85168624; Tel: +86-431-85168661*
[b] *Department of Basic Science, Jilin Jianzhu University, Changchun 130118, P. R. China*
[c] *Department of Chemistry and Chemical Biology, Rutgers University, Piscataway, New Jersey 08854, USA*

† Electronic supplementary information (ESI) available: Sample preparation, characterization details, the catalytic performance evaluation process, and N_2 adsorption–desorption, the valence state of Mn and O 1s spectra, and Arrhenius activation energy data. See DOI: 10.1039/c4cc00023d

This journal is © The Royal Society of Chemistry 2014

Published on 26 June 2014. Downloaded by Jilin University on 15/08/2017 03:09:29.

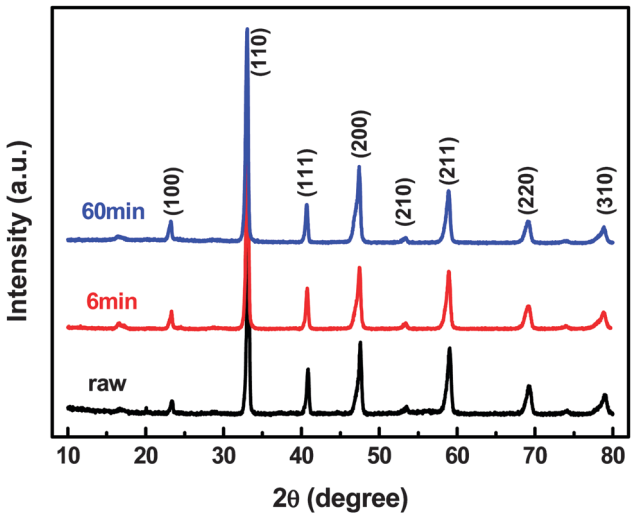

Fig. 1 X-ray diffraction patterns of $La_{0.5}Sr_{0.5}MnO_3$ for the raw sample without treatment (#1), and samples treated with dilute nitric acid solution for 6 min (#2) and 60 min (#3).

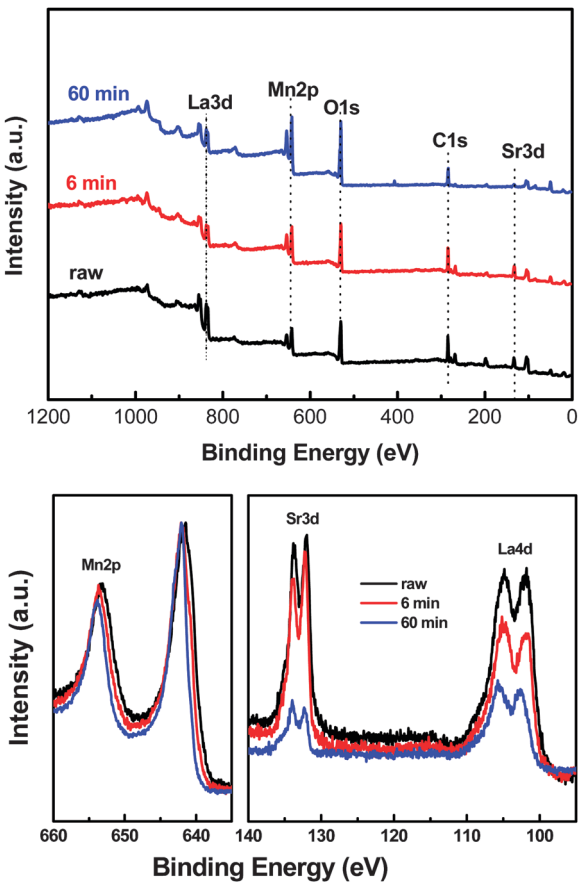

Fig. 2 XPS survey and Mn 2p, Sr 3d and La 4d spectra for the three samples #1, #2 and #3. (intensity of Sr 3d and La 4d were adjusted to the normalized Mn 2p.)

According to XPS quantitative analysis, the surface composition of the raw synthesized $La_{0.5}Sr_{0.5}MnO_3$ is 39.0 atom% of Mn/(La + Sr + Mn) (Fig. 2), which indicates La, Sr-enrichment on surfaces, in terms of ideal 50.0 atom% in EDS data. Change of La, Sr and Mn atomic ratios can be easily observed from the intensity variation in XPS survey spectra and detailed narrow scan core-level spectra of normalized Mn 2p and related La 4d and Sr 3d electrons. XPS quantitative results indicated that the surface has 46.8 and 67.5 atom% Mn for samples of 6 min and 60 min treatment. In contrast, the corresponding results of surface composition measurements by EDS show that the bulk Mn/(La + Sr + Mn) molar ratios (inset of Fig. 3) were 51.2%, 56.3% and 64.5% for sample #1, #2 and #3, respectively. These results indicated that the A-site atoms were successfully removed by wet-etching treatment, while EDS results also exhibited a quite smaller decrease of A site atoms compared to XPS results. It is obvious that La, Sr or Mn enrichment of $La_{0.5}Sr_{0.5}MnO_3$ particles was controlled from the surface to bulk process by selective wet-etching treatment time with a dilute acid at room temperature.

The scanning electronic microscope images revealed morphological evolution in an acidic environment, which improves the surface region from smooth in the ground raw material surface to a bit rough and fully rumpled surface, showing the possible reorganization of the surface structure (Fig. 3). The reason for selective removal of A-site atoms is the longer distance of La–O and Sr–O bonds than Mn–O bonds and the relatively high surface energy of the A–O bond. The surface electronic structure after treatment was improved, and the content of Mn^{3+} decreased and Mn^{4+} increased on the surface of Mn-rich particles. The ratios of $Mn^{4+}/(Mn^{3+} + Mn^{4+})$ are 40.2%, 62.8%, and 63.7% for samples #1, #2 and #3, respectively, as shown in Fig. S3 (ESI†). The additional Mn^{4+} promoted the formation of the surface oxygen vacancies. The production of Mn^{4+} at relatively high temperatures is important for the improvement of CO oxidation.[19,20]

The catalytic CO oxidation over the as-obtained samples was evaluated in a $CO–O_2–N_2$ stream. As shown in Fig. 4, for the conversion of CO into CO_2, T_{10} (the temperature of the conversion 10%) for sample #1, #2, #3 are 245, 169 and 158 °C and T_{50} (the half conversion temperature) are 340, 245 and 230 °C, respectively. To illustrate the relationship between enhanced catalytic behavior and the surface electronic structure, we schematically proposed the surface composition change, which indicates the elemental compositions, terminated layers on surfaces, and the corresponding surface evolution (Fig. 4). This means that the treated samples exhibited a much higher activity, which might be attributed to the presence of more active sites for creating a B-site (rich) terminated perovskite surface.

To further investigate the origin of different catalytic activity behaviors, temperature programmed reduction (TPR) of H_2 was tested to undestand the relative reducibility closely related to its catalytic performance (Fig. S1, ESI†). For the raw samples (#1), the peak in the range of 700–800 °C most likely corresponded to the reduction of the remaining Mn^{3+} to Mn^{2+}, meanwhile, the peak at about 507 °C can be attributed to the reduction of Mn^{4+} to Mn^{3+}. The peak shifted to lower temperatures, which may result from a single-electron reduction of Mn^{3+} located in a coordination-unsaturated microenvironment.[19] For samples

Published on 26 June 2014. Downloaded by Jilin University on 15/08/2017 03:09:29.

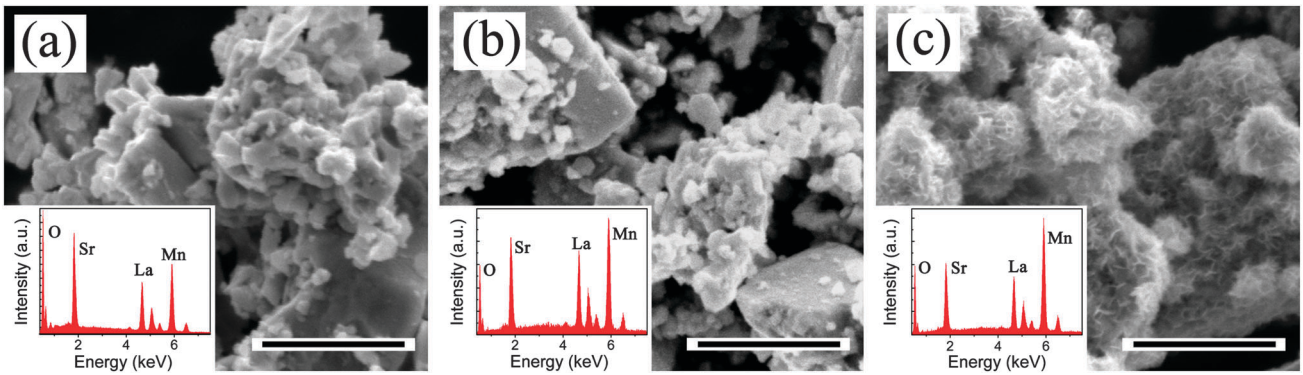

Fig. 3 SEM and EDS (inset) of $La_{0.5}Sr_{0.5}MnO_3$ (a) without treatment (1#), treated for (b) 6 min (2#) and (c) 60 min (3#). All scale bars are 1 μm.

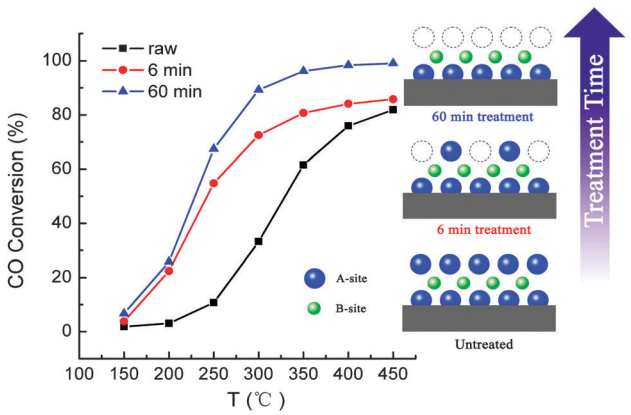

Fig. 4 Activity profiles of CO oxidation over the samples without treatment (raw), and treated with dilute nitric acid solution for 6 min and 60 min.

treated with dilute nitric acid solution for 6 (#2) and 60 min (#3), this situation may be favorable for the reduction of Mn^{4+} to Mn^{3+} at lower temperature as a result of the surface electronic structure change on the surface of Mn-rich particles. The peak at about 282 °C can be assigned to removal of nonstoichimetric excess oxygen accommodated within the lattice.[15] It is obvious that the position shifted to lower temperatures for the treated samples, indicating the better reducibility. The TPR results suggest[21] that high reducibility was achieved after the treatment with acid in this work, as it has been generally accepted that good redox property leads to excellent catalytic reactivity.[22]

O 1s XPS was measured to investigate the oxygen species on the surface or lattice of catalysts. Free oxygen vacancy was produced for whole reactivity,[23] which can serve as active sites and can increase the oxygen exchange rate, favoring the interaction with CO. The corresponding concentrations of O_{ad} (adsorbed oxygen species)/$O_{lattice}$ (lattice oxygen species) were obviously elevated (Fig. S3, ESI†), which was in good accordance with the observed catalytic activities and H_2-TPR results.

In this work the method of acid treatment created B-site (rich) terminated perovskite surfaces to overcome their fundamental flaw for catalytic activity, meanwhile, leading to an increased surface area (Fig. S2, ESI†). In order to eliminate the surface area effect, the apparent activation energy (E_a) of CO oxidation was calibrated (as shown in Fig. S4, ESI†). By comparing the E_a values of catalysts, one can evaluate their catalytic performance. The lower the E_a value is, the easier is the complete oxidation of CO.[24] The results clearly revealed that CO oxidation over three samples exhibits a surface-dependent catalytic activity similar to high-index planes dependence in some binary oxide systems (*e.g.* Co_3O_4 (ref. 25) and Cu_2O[26]), which are supposed to provide more active sites in either environments. However, the facets control for ternary perovskite oxides is much more difficult.[27] Therefore, this method applied here may give an alternative choice for enhancing surface dependent catalytic activities.

In summary, we have developed a reliable and ready method to create a B-site (rich) terminated perovskite surface for controllable selective wet-etching of perovskite-type oxides. Our wet-etching method can be applied to other perovskite-type oxides. We thus provide the fundamental engineering on metal oxide surfaces, which if properly controlled, can lead to radical enhancement of the catalytic activity.

This work was supported by the National Natural Science Foundation of China (Grants 90922034, 21131002, and 21201075) and Specialized Research Fund for the Doctoral Program of Higher Education (SRFDP Grant 20110061130005), and Natural Science Foundation of Jilin Province (Grants 20140520080JH).

Notes and references

1 S.-H. Yu, F. Tao and J. Liu, *ChemCatChem*, 2012, **4**, 1445–1447.
2 C.-H. Cui and S.-H. Yu, *Acc. Chem. Res.*, 2013, **46**, 1427–1437.
3 M. K. Debe, *Nature*, 2012, **486**, 43–51.
4 Y. Li and W. Shen, *Chem. Soc. Rev.*, 2014, **43**, 1543–1574.
5 W. F. Libby, *Science*, 1971, **171**, 499–500.
6 S. Royer and D. Duprez, *ChemCatChem*, 2011, **3**, 24–65.
7 D. Neagu, G. Tsekouras, D. N. Miller, H. Ménard and J. T. S. Irvine, *Nat. Chem.*, 2013, **5**, 916–923.
8 J. M. D. Tascon and L. G. Tejuca, *J. Chem. Soc., Faraday Trans.*, 1981, **77**, 591–602.
9 C.-C. Tsai and H. Teng, *Chem. Mater.*, 2006, **18**, 367–373.
10 D. Fodor, L. Pacosová, F. Krumeich and J. A. von Bokhoven, *Chem. Commun.*, 2014, **50**, 76–78.
11 W. Sugimoto, M. Shirata, Y. Sugahara and K. Kuroda, *J. Am. Chem. Soc.*, 1999, **121**, 11601–11602.
12 H.-Z. Geng, K. K. Kim, K. P. So, Y. S. Lee, Y. Chang and Y. H. Lee, *J. Am. Chem. Soc.*, 2007, **129**, 7758–7759.

 This journal is © The Royal Society of Chemistry 2014

13 F. Li, Y. Zhan, T.-H. Lee, X. Liu, A. Chikamatsu, T.-F. Guo, H.-J. Lin, J. C. A. Huang and M. Fahlman, *J. Phys. Chem. C*, 2011, **115**, 16947–16953.
14 X. Chu, K. Huang, M. Han and S. Feng, *Inorg. Chem.*, 2013, **52**, 4130–4132.
15 K. Huang, X. Chu, W. Feng, C. Zhou, W. Si, X. Wu, L. Yuan and S. Feng, *Chem. Eng. J.*, 2014, **244**, 27–32.
16 C. N. Borca, B. Xu, T. Komesu, H.-K. Jeong, M. T. Liu, S. H. Liou and P. A. Dowben, *Surf. Sci.*, 2002, **512**, L346–L352.
17 H. Dulli, P. A. Dowben, S.-H. Liou and E. W. Plummer, *Phys. Rev. B: Condens. Matter Mater. Phys.*, 2000, **62**, 629–632.
18 Z. Cai, Y. Kuru, J. W. Han, Y. Chen and B. Yildiz, *J. Am. Chem. Soc.*, 2011, **133**, 17696–17704.
19 F. Teng, W. Han, S. Liang, B. Gaugeu, R. Zong and Y. Zhu, *J. Catal.*, 2007, **250**, 1–11.
20 S. Liang, F. Teng, G. Bulgan and Y. Zhu, *J. Phys. Chem. C*, 2007, **111**, 16742–16749.
21 J. L. Fierro, J. M. Tascón and L. G. Tejuca, *J. Catal.*, 1985, **93**, 83–91; P. K. Gallagher, D. W. Johnson and E. M. Vogel, *J. Am. Ceram. Soc.*, 1977, **60**, 28–31.
22 T. Nakamura, M. Misono and Y. Yoneda, *J. Catal.*, 1983, **83**, 151–159.
23 N. A. Merino, B. P. Barbero, P. Eloy and L. E. Cadús, *Appl. Surf. Sci.*, 2006, **253**, 1489–1493.
24 H. Arandiyan, H. Dai, J. Deng, Y. Liu, B. Bai, Y. Wang, X. Li, S. Xie and J. Li, *J. Catal.*, 2013, **307**, 327–339.
25 X. Xie, Y. Li, Z.-Q. Liu, M. Haruta and W. Shen, *Nature*, 2009, **458**, 746–749.
26 M. Leng, M. Liu, Y. Zhang, Z. Wang, C. Yu, X. Yang, H. Zhang and C. Wang, *J. Am. Chem. Soc.*, 2010, **132**, 17084–17087.
27 C. Hou, W. Feng, L. Yuan, K. Huang and S. Feng, *CrystEngComm*, 2014, **16**, 2874–2877.

Published on 26 June 2014. Downloaded by Jilin University on 15/08/2017 03:09:29.